





Electric field assisted-unidirectional hybrid films of carbon nanotubes and liquid crystal polymer for light modulation

Weiwei Tie, Surjya Sarathi Bhattacharyya, Zhi Zheng, Kyung Jun Cho, Tae Hyung Kim, Young Jin Lim & Seung Hee Lee


To cite this article: Weiwei Tie, Surjya Sarathi Bhattacharyya, Zhi Zheng, Kyung Jun Cho, Tae Hyung Kim, Young Jin Lim & Seung Hee Lee (2020) Electric field assisted-unidirectional hybrid films of carbon nanotubes and liquid crystal polymer for light modulation, *Liquid Crystals*, 47:3, 317-329, DOI: [10.1080/02678292.2019.1647572](https://doi.org/10.1080/02678292.2019.1647572)


To link to this article: <https://doi.org/10.1080/02678292.2019.1647572>

 View supplementary material [↗](#)

 Published online: 11 Aug 2019.

 Submit your article to this journal [↗](#)

 Article views: 114

 View related articles [↗](#)

 View Crossmark data [↗](#)



Electric field assisted-unidirectional hybrid films of carbon nanotubes and liquid crystal polymer for light modulation

Weiwei Tie^{a,b}, Surjya Sarathi Bhattacharyya^c, Zhi Zheng^{a,b}, Kyung Jun Cho^d, Tae Hyung Kim^d, Young Jin Lim^d and Seung Hee Lee^d

^aKey Laboratory of Micro-Nano Materials for Energy Storage and Conversion of Henan Province, School of Advanced Materials and Energy, Institute of Surface Micro and Nanomaterials, Xuchang University, Xuchang, China; ^bHenan Joint International Research Laboratory of Nanomaterials for Energy and Catalysis, Xuchang University, Xuchang, China; ^cDepartment of Physics, Asutosh College, Kolkata, India; ^dApplied Materials Institute for BIN Convergence, Department of BIN Convergence Technology and Graduate School of Flexible & Printable Electronics Engineering, Chonbuk National University, Jeonju, South Korea

ABSTRACT

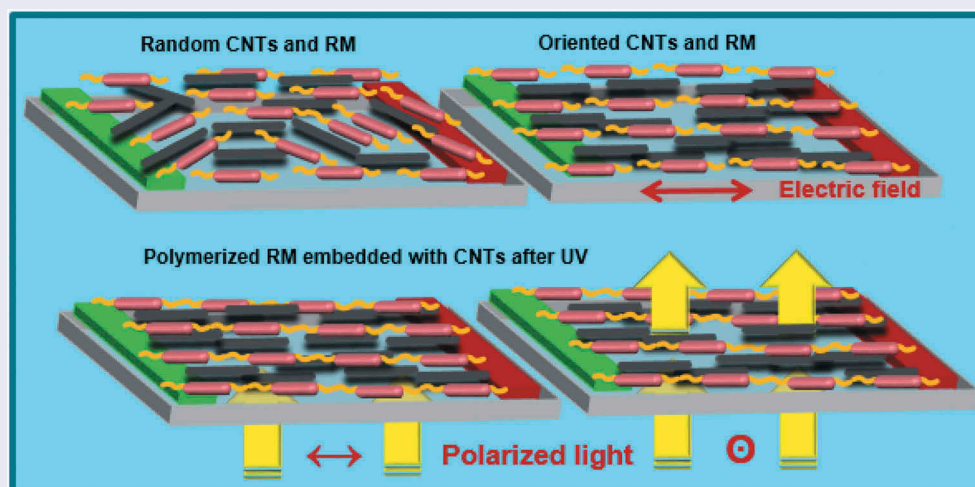
To develop stable polymer films which had high orientational ordering of carbon nanotube for polarization-dependent light modulator, we present a new concept for electric-field induced alignment of mesogenic carbon nanotubes (m-CNTs) in reactive mesogen host (RMS) fixed by ultraviolet (UV) polymerization. Covalent modification of m-CNTs was performed using structure-tailored mesogenic units [4-(6-hydroxyhexanoly)-4'-carbonitrile, PCNOH] in esterification reaction based on 100–500 nm long CNTs shortened by acid oxidation cutting, confirmed through ¹H NMR, FT-IR, Raman and XPS spectroscopy. Dynamic orientation of m-CNTs in soft m-CNT/RMS composite without aggregates was observed on a large scale by polarized optical microscopy, in which m-CNTs aligns along the electric field direction. It was reasonable the mesogenic segments introduced onto m-CNTs weakened van der Waals interactions between the nanotubes by increasing steric repulsion, and then effectively improved the favourable affinity of m-CNTs with RMS molecules. Direct UV-induced polymerization of RMS molecules stabilized the orientational ordering of m-CNTs confirmed by Raman spectroscopy, and the obtained film also exhibited anisotropic light absorption depending on the polarization direction of an incident light. The facile methodology described in this study to generate oriented films of m-CNTs-in-RMS broadened the scope of potential applications of modulator devices and versatile functional composites with anisotropic physical properties.

ARTICLE HISTORY

Received 21 June 2019
Accepted 21 July 2019

KEYWORDS

Carbon nanotubes; reactive mesogen; electric-field induced orientation; ultraviolet polymerization



Graphical illustration of a conceived light modulator utilizing m-CNT/RM.

1. Introduction

Carbon nanotubes (CNTs) are micrometre-sized cylindrical tubes of nanometric diameter consisting of

a single or few layers of graphene sheets. Uniformly aligned CNTs exhibit extremely strong optical anisotropy along with both the parallel and perpendicular directions of the tube axis due to their peculiar

geometric shape [1–4]. Uniform orientation is necessary for many newly proposed CNT materials and devices. Hence, techniques of organizing CNTs in a uniform manner are required to generate these innovative properties on a macroscopic scale. However, CNTs tend to form aggregates due to substantial van der Waals attractive interaction that prevents uniform alignment of the nanostructures [5,6].

Recently, various strategies of aligning CNTs have been reported [6–16], in which the CNTs are first dispersed with the help of various dispersants and then sequentially align them utilizing a single method, such as those based on electromagnetic fields, shear flowing, mechanical stretching, and liquid crystal (LC) phases. Shortcomings and limitations do remain till date regarding the development of a single unique method of orienting CNTs. Practical application of CNTs is hindered by low doping content in appropriate solvent, uncontrollable aligning direction, and undesirable aligning mode. Therefore, methods of controlling CNT orientation in an efficient and comprehensive manner are keys for fabricating large-scale functional film and electronic devices.

Extensive studies [17–19] have successfully demonstrated electric field-induced orientation of single CNT aggregates in thermotropic nematic LCs. This has attracted widespread interest for use as a tunable polarizer device since an incident visible light is selectively absorbed depending on the polarization direction of the light propagating either parallel or perpendicular to the longitudinal direction of CNTs in LC host [18–20]. However, previous studies have revealed competition between the applied field and van der Waals interactions between CNTs within aggregates is of vital importance for field-dependent alignment of CNT aggregates. In addition, most LCs are insoluble hosts for CNTs [9,20,21], causing bulk doping and subsequent macro-orientation of CNTs to be very difficult.

In general, modifying the functionality of CNTs by attaching various groups onto their sidewalls will weaken van der Waals interactions between CNTs and promote their dispersion into the LC host [22–24]. Previous studies have demonstrated relatively easy electric field-induced alignment of CNTs through functionalization of carboxylic and other oxygen-containing functional groups named as carboxylic CNTs (c-CNTs), in which the functional groups attached to the graphene-like surface of c-CNTs reduced interactions between CNTs through either electrostatic repulsion if they were charged or steric repulsion by creating space between the tubes that reduces the tube-tube van der Waals interactions [18,23,24]. In the present study, we have considered introducing one long-chain mesogen segment onto shorted carboxylic CNTs to enhance dispersion and alignment. This method is expected to improve

the affinity of CNTs for the reactive mesogen (RMS) host due to the structural similarity of the CNTs with RMS and reduce the van der Waals interactions between the tubes due to increased steric repulsion from structural discrepancies [18,22–24]. It is therefore imperative to understand the effect of reducing the van der Waals interactions between tubes based on the field-induced orientation of CNTs in RMS host. Briefly describing, CNTs were first modified with carboxylic groups named as c-CNTs and then chemically esterified with 4-cyano-4'-hexylylbiphenol to obtain m-CNTs. These m-CNTs were tailored by covalently attaching mesogenic units using a flexible spacer linking onto the carboxylic CNTs. Larger spacers were introduced between the tubes of the m-CNTs compared to CNTs only treated with acid and thus it increased compatibility with the RMS host through structural similarity. Therefore, we expect a significant improvement in the dispersion of m-CNTs in the RMS host and enhanced field-induced alignment of CNTs owing to mesogenic CNTs.

In this paper, a convenient process of uni-directional orientation of CNTs has been reported for fabrication of polarizing films. Specifically, the electric field is utilized to align long axes of m-CNTs in conjunction with orientation of reactive liquid crystalline molecules. Next, the UV-solidification method is used to retain the nanotube alignment through crosslinking of liquid crystalline monomers under applied electric field. This technique thus provides a method of preparing very large, thin films of embedding aligned nanotubes on various suitable substrates by electric field and UV irradiation processing. The electrical field-induced macroscopic arrangement and orientation of the m-CNTs are detected and verified using standard characterizing methods, including polarized optical microscopy and Raman spectroscopy. The alignment of the m-CNTs after UV irradiation in a field-off state and their selective light absorptions are also discussed.

2. Experimental

2.1. Materials

Multi-walled carbon nanotube (MWCNT) sample was supplied by the Aladdin Co. Ltd. in powder form with the CNTs having outer diameters and lengths ranging from 3 to 6 nm and 0.5 to 2 μm , respectively. Pyridine (analytical grade), 4'-hydroxy-4-biphenylcarbonitrile (99%), 6-Chloro-1-hexanol (98%), and N, N-dimethylaminopyridine (98%) were obtained from Aladdin Co. Ltd. and used without further treatment. A planar aligned anisotropic polymer film of Reactive mesogens (RMS03-013C, Merck-Japan) is realized after spin-coating at 3000 rpm for

30 s, drying, and UV curing on suitable substrate using literature reported methods [25].

2.2. Preparation of mesogenic moiety

A mixture of 4-hydroxy-4'-cyanobiphenyl (0.7810 g, 4 mmol), K_2CO_3 (1.6323 g, 11 mmol), and 6-Chloro-1-hexanol (0.5621 g, 4 mmol) in 2-butanone (150 mL) was refluxed for 72 h in an argon atmosphere. After evaporation of the solvent under reduced pressure, the residue was dissolved in chloroform (100 mL) and washed with water (100 mL) several times. The organic layer was concentrated in vacuo and then dried at 50°C in a vacuum oven.

2.3. Preparation of carboxylic CNTs

To add carboxylic groups onto CNT sidewalls, about 0.5 g of MWCNT powder was refluxed with a concentrated mixture of 80 ml H_2SO_4 (98%)/ HNO_3 (68%) at a 3:1 (v/v) ratio in a 250 ml round-bottom flask for 8 h. The reactant was placed into the 200 ml and then filtered through a 0.2 μm anodic alumina membrane (Whatmann). Several rounds of washing in deionized water were performed until the pH reached ~ 7 , and then the sample was dried in an oven at 100°C to yield carboxylic CNT powder (c-CNTs).

2.4. Preparation of mesogenic CNTs

Carboxylic CNTs were further modified to make them more compatible with the reactive mesogen monomer mixture. A mixture of the abovementioned carboxylic CNTs (0.2 g) and thionyl chloride (80 ml) was refluxed for 24 h and then excess thionyl chloride was evaporated at reduced pressure. Next, the above-mentioned CNTs were carefully dried in vacuo, flushed with argon, and then treated with a mixture of dry pyridine (1 ml) and DMAP (3 mg) in dry dichloromethane (25 ml). After refluxing for 24 h, the mixture was filtered through PTFE filters and washed with water and chloroform. Finally, the product was dried in a vacuum oven at 60°C to yield mesogenic CNTs (m-CNTs). Scanning electron microscopy images of the m-CNTs are shown in Fig. S1.

2.5. Preparation of thin mesogenic CNT/RMS composite films

To investigate and compare the influence of the functional mesogen units on the dispersion of CNTs, either carboxylic or mesogenic CNTs (~ 0.2 wt %) were dispersed in the positive dielectric anisotropic nematic LC ($\Delta\epsilon = +14$) viz. ZLI-4535 (Merck-Japan) and sonicated

for 30 min. The effect of the above-mentioned functional modification was scrutinized in the present investigation. To observe the dispersion morphology of each type of nanotube in nematic LC, an interdigitated electrode made of aluminium metal was patterned on bottom glass substrate. The interdigital electrodes were 10 μm wide with intra-electrode interval maintained at either 20 or 40 μm and bare glass was used as the top substrate. The alignment layer viz. SE-6514 (Nissan Chemicals) was spin-coated on both substrates, and then baked at 200°C for 1 h to evaporate solvent and adhere to the substrates. Additionally, to achieve homogeneous alignment of nematic LC molecules, rubbing was performed at a 90° rubbing angle with respect to the electrode direction. Finally, sandwiched cells with thickness of about 80 μm were constructed. The test cells were filled with the NLC-CNT mixture using a capillary action technique at room temperature. Analysis of the dispersion of the carboxylic and mesogenic CNTs shown in the subsequent sections demonstrates the m-CNTs with attached additional mesogenic groups possessed distinct dispersion properties compared to the carboxylic CNTs.

Due to ease dispersion of mesogenic CNTs in LCs, a well-dispersed mixture of mesogenic CNTs (0.2 wt%) in RMS was prepared following the aforementioned procedure. To observe in-plane field-dependent behaviour of m-CNTs in reactive mesogen, the device was prepared following the above-mentioned procedure with just one bottom substrate without rubbing process. Figure 1 displays a schematic fabrication technology for the electrically oriented CNT polarization device. The homogenous m-CNT/RMS composite mixture was spin-coated onto the patterned electrode substrate pre-coated with alignment layer at 800 rpm for 2.3 s and 3000 rpm for 30 s and then oven dried at 70°C for 2 min to remove residual solvent, resulting in the formation of a planar aligned anisotropic polymer film. Before applying the field, the m-CNTs mixture with RMS molecules were randomly aligned (a). As an in-plane electric field was applied, the soft composite of the m-CNTs and mesogenic molecules became completely orientated along the field direction (b). UV irradiation (25 mw/cm^2) was used to fabricate photo-polymerized films at field-on state (c). After UV irradiation, the electric field was removed and a stable aligned film in a field-off state was realized (d).

2.6. Characterization

The morphology of the functionalized m-CNTs was examined by field emission-scanning electron microscopy (SU8020, Hitachi UHR FE-SEM). The samples were prepared for microscopic observation by mixing either type of CNTs in chloroform and then sonicating

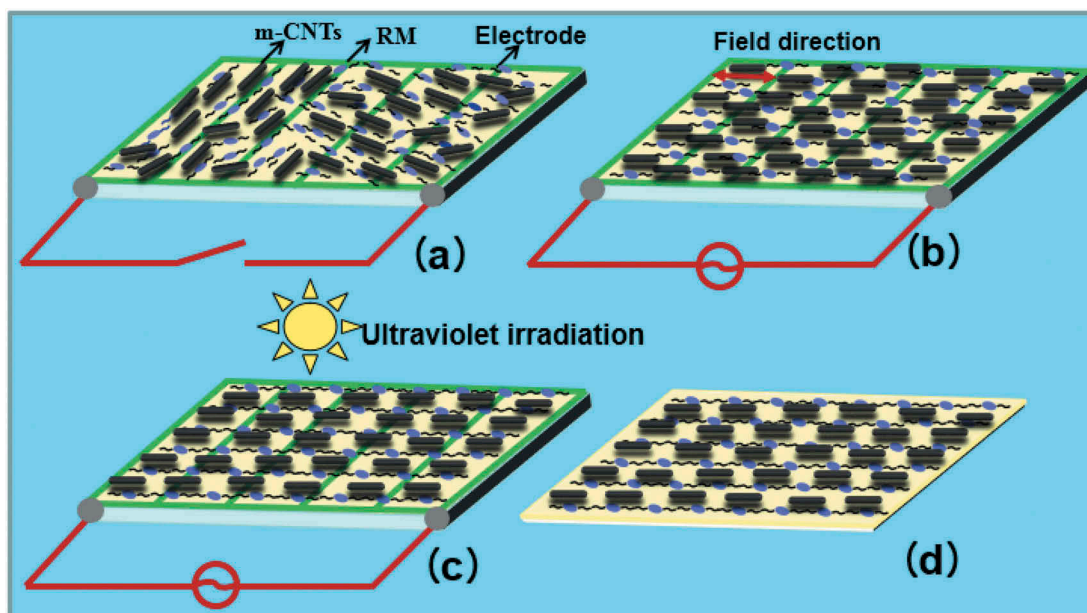


Figure 1. (Colour online) Schematic processing steps for fabricating CNT based optical polarizer with electric-field assistance (a: coating soft composite on the substrate with interdigitated electrodes, b: unidirectional assembly of m-CNTs and RM by applying an electric field, c: fixation of orientational ordering of m-CNT by polymerization of RM with ultraviolet irradiation, and d: Realized functional hybrid film in the absence of an electric field).

for 10 min. Then, the resulting supernatant was drop-dried on a clean glass. Nuclear magnetic resonance (^1H NMR) spectra were carried out by Bruker Avance III 400. Fourier-transform infrared spectroscopy (FT-IR) spectra were obtained using a Perkin Elmer Spectrum-GX, while X-ray photoelectron spectroscopy (XPS) was carried out using an XPS spectrometer (Thermo escalab 250XI, USA) with Al-K α radiation ($h\nu = 1486.6$ eV). The charge compensation was corrected with carbon 1 s to 284.6 eV. Thermogravimetric analyses (TGA) were performed on a TGA2050 (TA Instruments) at a heating rate of 15°C/min to a maximum of 700°C. Nitrogen was used as the purge gas at a flow rate of 60 mL/min. Raman spectroscopy was performed using Renishaw inVia with laser excitation at 532 nm through a 50 \times objective lens. For orientation study, the intensity of the field-treated hybrid film was measured by Renishaw inVia as a function of polarization of incident light with laser excitation at 532 nm [24]. The optical textures of the prepared samples were observed by optical microscopy (Nikon DXM1200) while applying a sinusoidal field at a fixed frequency.

3. Result and discussion

We have pursued covalent functionalisation of CNTs by attaching a functional mesogenic moiety as dispersion promotor onto nanotube sidewalls [23] to generate uniformly dispersed and oriented CNTs in traditional commercial LCs. The synthesis of m-CNTs containing mesogenic units (PCNOH) is illustrated in Figure 2. This mesogenic unit (PCNOH) is tailored by combining a cyanobiphenyl unit (BCNOH) via a flexible 6-chlorohexanol spacer through Williamson reactions. The chemical structure of PCNOH is confirmed by ^1H NMR (Figure 3) and FT-IR spectroscopy (Figure 4). The ^1H NMR spectrum of PCNOH in Figure 3 shows aromatic proton peaks at 7.69–7.65, 7.65–7.61, 7.55–7.49, and 7.00–6.96 ppm and aliphatic proton peaks at 4.06–3.96, 3.70–3.62, and 1.85–1.38 ppm. Chemical shifts located at 7.69–7.65 and 7.65–7.61 ppm are attributed to proton signals at the ortho and meta positions of the benzene ring corresponding to a CN moiety. Chemical shifts located at 7.55–7.49 ppm and 7.00–6.96 ppm are assigned with the proton signals of the meta and ortho positions of

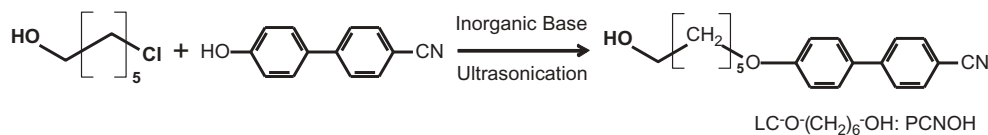


Figure 2. Schematic route of mesogenic unit.

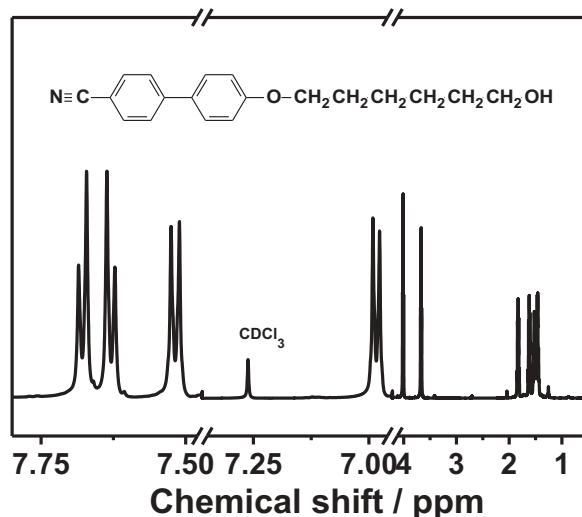


Figure 3. (Colour online) ^1H NMR spectra of PCNOH.

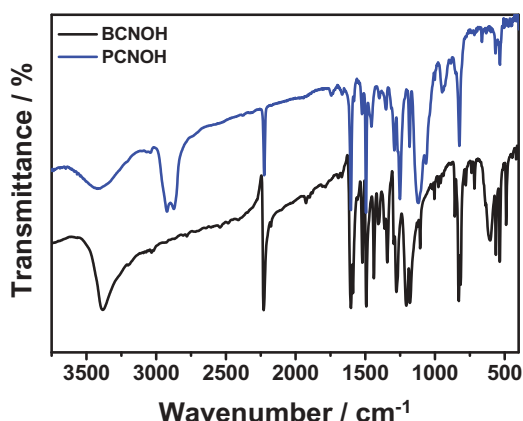


Figure 4. (Colour online) FT-IR spectra of PCNOH and BCNOH.

the biphenyl ring corresponding to the adjacent $-\text{OCH}_2$ moiety. Proton signals from OCH_2 - moieties connected to biphenyl and $-\text{OH}$ groups are observed as doublets at 4.06–3.96 ppm and 3.70–3.62 ppm. The proton signals from four $-\text{CH}_2$ groups were observed at 1.38–1.85 ppm.

Chemical structure analysis of the mesogenic moiety yields strong evidence for target design completely consistent with similar investigations reported earlier [23]. In the FT-IR spectra of PCNOH and BCNOH shown in Figure 4, both generate similar absorption bands around 1604 cm^{-1} and 2223 cm^{-1} , which are assigned to characteristic peaks of asymmetric stretching of $\text{C}=\text{C}$ of biphenyl groups and $\text{C}-\text{N}$ of cyano groups. However, new peaks appeared at 2919 and 2866 cm^{-1} can be ascribed to $\text{C}-\text{H}$ stretching of methyl groups (CH_2) [26]. Therefore, it is reasonable to conclude the long methyl chain is successfully reacted to the cyanobiphenyl unit, further supporting the designed structure of the target product.

FT-IR spectroscopy is carried out for the c-CNTs and m-CNTs to identify their functionality as shown in Figure 5(a). As described earlier, the c-CNTs are prepared through acid-sonochemical oxidation of pristine MWCNTs [27] and the m-CNTs are further functionalized with the above-mentioned mesogenic units. Absorption bands for the CNT backbone around

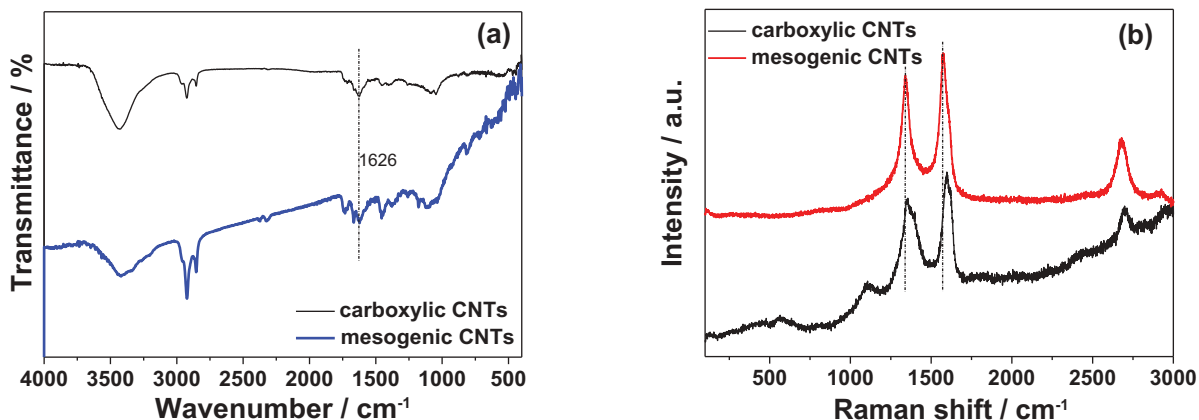


Figure 5. (Colour online) FT-IR (a) and Raman spectra (b) of carboxylic and mesogenic CNTs.

1620 cm^{-1} (C = C stretching) for c-CNTs and m-CNTs are found on both types of tubes and originated from the inherent structure of the CNTs. However, the shift of carbonyl absorption peak (C = O stretching) from around 1724 cm^{-1} for c-CNTs to around 1735 cm^{-1} for m-CNTs indicates the changes in their adjacent groups, and the characteristic peaks appeared around 1451 cm^{-1} and around 2825–2990 cm^{-1} obviously increases due to stretching vibrations of biphenyl rings and asymmetric and symmetric CH_2 stretching of aliphatic chains. The variation of characteristic absorption is mainly attributed to the introduction of the structure-tailored mesogenic unit (PCNOH) in m-CNTs compared to those of c-CNTs. The results clearly indicate functional mesogenic groups are successfully introduced onto the surface of the CNTs through esterification of carboxyl groups on CNTs and hydroxyl groups on PCN, in agreement with earlier investigations [27–29].

Raman spectroscopy is also utilized to investigate the carbon structure of each type of prepared CNTs. Figure 5(b) shows the Raman spectra of c-CNTs and m-CNTs. The dominant Raman features around 1350 cm^{-1} for c-CNTs and 1342 cm^{-1} for m-CNTs are amorphous or disordered non-graphitic carbon structures (D-band), while those at 1597 cm^{-1} for c-CNTs and 1574 cm^{-1} for m-CNTs are from in-plane tangential stretching of the carbon-carbon bonds (G-band) in graphene sheets. The peak shifting of the G band from c-CNT to m-CNTs clearly indicates strong charge transfer from the carbon sidewalls to related functional groups, indicating different functional groups are attached to the CNT sidewalls due to the covalent grafting of mesogenic units with c-CNTs via esterification [18,30]. Additionally, the I_D/I_G ratios of the c-CNTs and m-CNTs are 0.82 and 0.94, respectively. This also indicates chemical covalent modification with

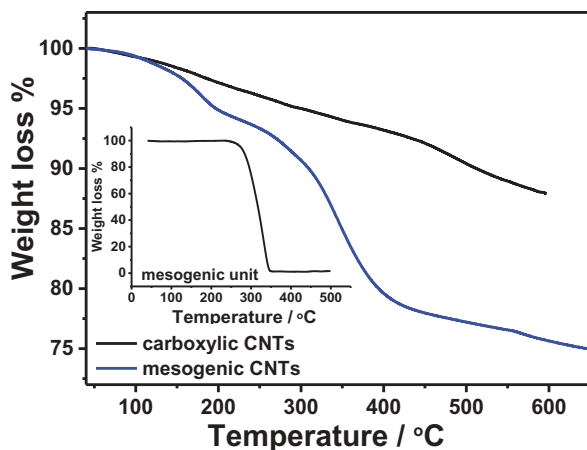


Figure 6. (Colour online) TGA thermograms of carboxylic and mesogenic CNTs.

different functionalisation onto the nanotube sidewalls for each kind.

TGA is employed to obtain thermogravimetric data from a thermogram to further characterize different functional groups attached to the sidewalls of each type of CNT. Figure 6 depicts the TGA results for c-CNTs and m-CNTs, where the inserted graph represents the thermogravimetric information from the mesogenic unit of PCNOH. Compared to c-CNTs, the m-CNTs display three-stage weight loss. Both CNT types have similar initial weight loss around $\sim 100^\circ\text{C}$ associated with physical desorption of water molecules on the CNTs surface. For m-CNTs, the second weight loss occurs around 250–300°C due to the loss of functional groups, such as mesogenic moieties, from the surface of the m-CNTs. This decomposition temperature range is lower than that of m-CNTs (around 400–450°C). Covalent attachment of mesogenic moieties onto c-CNTs is believed to decrease the decomposition temperature range from 400–450°C to 250–300°C. The third weight loss starts around 500°C and continued up to 600°C. Finally, it is found about 15% mesogenic units are covalently linked onto m-CNTs from the char yield from the TGA results, because a complete weight loss is observed for mesogenic units at $\square 350^\circ\text{C}$, presumably due to thermal evaporation [31,32]. The TGA results provide a strong evidence for attachment of distinct functional groups onto sidewalls of c-CNTs and m-CNTs.

X-ray photoelectron spectroscopy (XPS) is performed to gain further insight into the chemical composition and bond configuration changes of m-CNTs associated with the reaction shown in Scheme 1. Figure 7 presents the survey spectra of the c-CNTs (a, c) and m-CNTs (b, d). As expected, only C1s and O1s peaks are seen for c-CNTs (a) in the XPS spectrum. However, the appearance of the N1s (408.9 eV) peaks, accompanied by the increased ratio of O1s peak with respect to the C1s peak, in the m-CNT XPS results (b) indicates covalent bonding of tailored mesogenic groups of PCNOH onto CNT sidewalls is successful. Analyses of bond configuration changes in detail are executed in the high-resolution C1s core-level spectra of the c-CNTs (c) and m-CNTs (d) using a peak fit program and peak deconvolution. In the C1s spectrum, the four fitted peaks are found at 284.7, 285.7, 286.7 and 291.2 eV for c-CNTs. However, the five fitted peaks pertain to m-CNTs appear at 284.7, 285.1, 286.1, 289.2 and 291.6 eV. For both types of CNTs, the peaks around 284.7 eV are attributed to the sp^2 graphitic structure [33], while the peaks around 285.7 eV and 286.7 eV for c-CNTs and 285.1 eV, 286.1 eV and 289.2 eV for m-CNTs with shifting can be assigned to the carbon atoms attached to different oxygen-containing moieties of C-C and C-O/C = O bands [34,35].

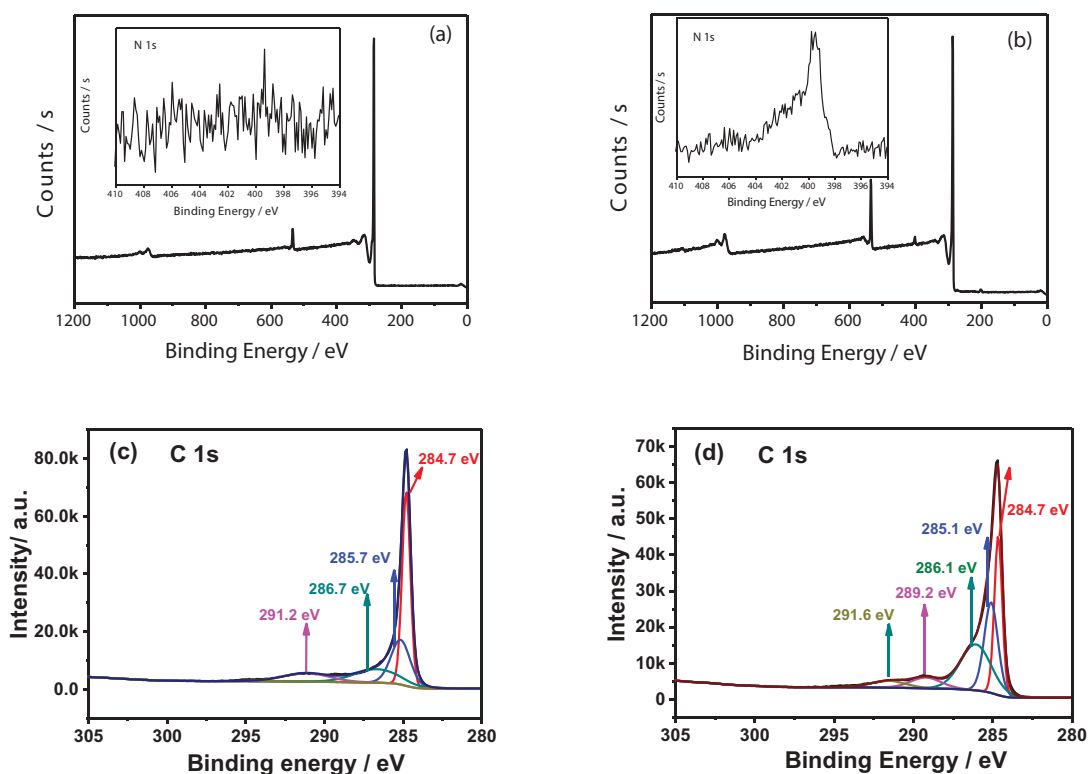


Figure 7. (Colour online) XPS survey spectra of carboxylic CNTs (a) and mesogenic CNTs (b) and high-resolution XPS spectra of C 1s of carboxylic (c) and mesogenic CNTs (d).

Compared with c-CNTs, the shifting of a component from 291.2 eV for c-CNTs to 291.6 eV for m-CNTs is observed due to the variation of π - π^* shake-up satellite [36], and the obvious increase in the peak intensity at 286.1 eV for the m-CNTs could be ascribed to the appearance of a new $C \equiv N$ bond [37]. Additionally, the red-shifting of the peak position to a lower energy for the $C = O$ bond of the m-CNTs indicates a chemical reaction between c-CNTs and functional mesogenic unit [24]. Finally, the obvious shift of the π - π^* transition loss peak clearly reveals a strong interaction between CNTs and functional molecules in m-CNTs or the functional

molecules in m-CNTs [34]. XPS analysis of each type of CNT clearly evidences the functionality of mesogenic units onto CNT sidewalls and the effective interactions of functional molecules between m-CNTs.

Figure 8 shows optical microscopic textures of the constructed cells for each type of CNT through 20 \times objective lens. Distinct dispersion characteristics of c-CNTs and m-CNTs are observed clearly. The absence of m-CNTs aggregates in microscopic image indicates the aggregate size is smaller than the visible wavelength range beyond the optical microscopic limits of resolution. It is well known that normal CNTs are strongly anchored to

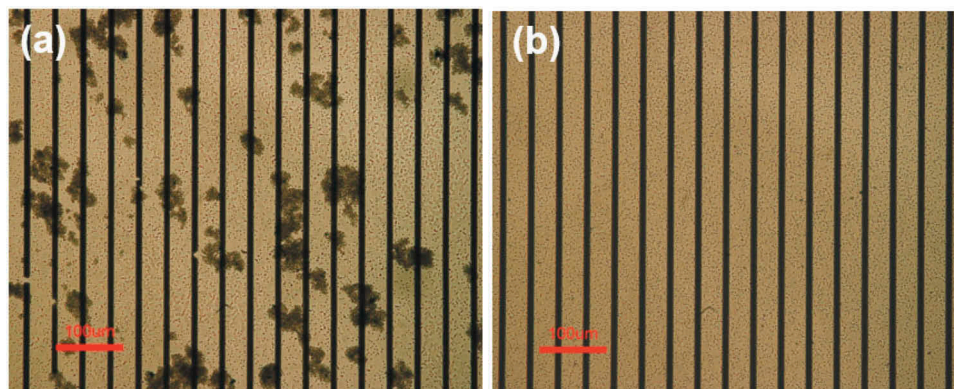


Figure 8. (Colour online) Optical microscopy images of carboxylic CNTs (a) and mesogenic CNTs (b) in mesogenic medium.

each other due to their graphitic-like surface induced π - π interactions [9,16], and then normal CNTs in liquid crystal (LC) medium will assemble a random network of contacting aggregates, which consists of stochastically arranged nanotubes and a 'shell' ('coat') of incorporated and adjacent nematic molecules [38]. For the modified m-CNTs, the rod-like mesogenic unit linked with the polar and flexible spacer has been introduced, in which the polar and flexible spacer introduced is similar to introduce a nanoscale incompatibility that separates the CNTs from the mesogenic moieties. Compared to normal CNTs, by incorporating the rod-like mesogenic unit modified by the polar and flexible spacer, the dispersion of the m-CNTs in LC has been improved because the m-CNTs have good compatibility with LC medium due to the rod-like mesogenic unit, more importantly, the m-CNTs have been further separated with each other due to their stronger steric effect of the polar and flexible spacer. The m-CNTs/LC system have become looser and their fractal characteristic are more obvious [24]. Here, covalent introduction of rod-like mesogenic units modified by the polar and flexible spacer onto m-CNTs efficiently improves the interface interaction between each CNTs of m-CNTs and liquid crystal medium or functional mesogenic unit in m-CNTs, and then greatly stabilizes the interface interaction between CNT and LC, confirmed by the abovementioned Raman and XPS analysis.

Obviously, further functionalisation of c-CNTs with structure-tailored mesogenic units (PCNOH) increases the compatibility of m-CNTs with mesogenic host and then decreases their aggregate size due to their similar molecule structures. Using the correct combination of these components, we have generated uniformly dispersed and stable m-CNTs in a standard commercial nematic LC mixture, even though LC alone is a poor CNT solvent. As described above, further improvement in m-CNT dispersion is achieved using an extra reaction

between c-CNTs and PCNOH groups. Therefore, to direct the field-induced orientation, m-CNTs are utilized to develop nanocomposites in combination with a reactive mesogen composed of UV-crosslinkable acrylate material (RMS) [25]. RMS is a commercial LC monomer with reactive functionalities which can align its long axis spontaneously parallel to the applied field direction. Dispersion processing of up to 0.2 wt% m-CNTs into reactive mesogen is easily carried out assisted by ultrasound for 60 min without the use of other solvents. After centrifugation of mixture at 2000 rpm, there is no appearance of any sediment even after 24 h. Its orienting procedure is also very convenient since it does not require any surface treatment prior to mixture alignment on a substrate surface. For field-assisted hybrid films, the substrates with interdigitated electrodes on one side are cleaned with pure water and acetone and dried through purging of nitrogen gas for several times.

Figure 9 exhibits the optical microscopic images showing a representative large-scale m-CNT alignment as a function of applied electric field strength at 60 Hz frequency. Before the field applied, the m-CNTs are uniformly dispersed though they are entangled into a few micrometre-sized aggregates under optical observation, demonstrating good compatibility of m-CNTs with mesogenon molecules. After applying the field of $4 V_{\text{rms}}/\mu\text{m}$, m-CNTs stretch along the field direction, changing their macroscopic shape from sphere to rod. The macroscopic orientation of the m-CNTs could be easily realized via the observed elongated traces of the formed CNT bundles in the microscopic image.

The field-induced stretching and alignment behaviour of CNTs has been studied in previous studies [17–20] and can be explained by considering applied electric field-induced dipolar reordering of CNTs from a random to a field-directed linear form. After applying an electric

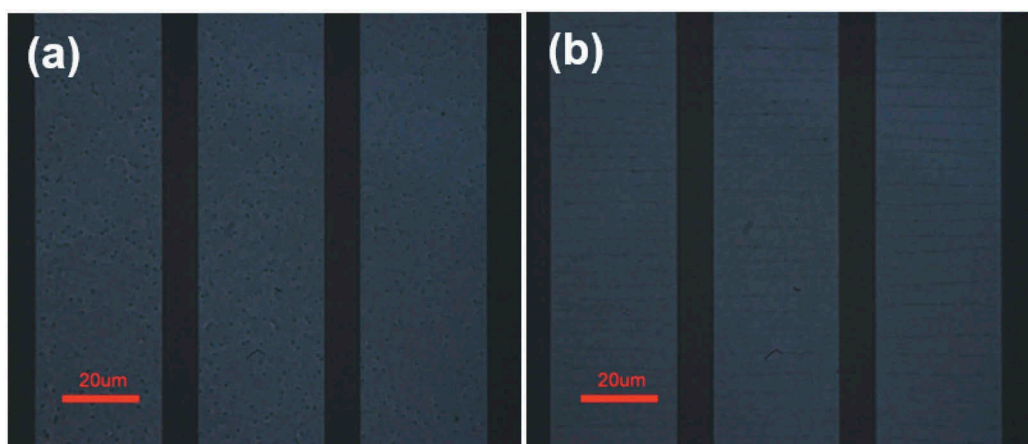


Figure 9. (Colour online) In-plane field-induced orientation of mesogenic CNTs at initial (a) and field-on states (b).

field, CNTs in host medium experience the net force \vec{F}_{elec} given by

$$\vec{F}_{elec} = -q\vec{E} + \vec{p} \cdot \nabla \vec{E} \quad (1)$$

where ' \vec{p} ' means the induced dipole moment and ' q ' means the charge induced on the CNT aggregate under an electric field ' \vec{E} '. The first term ' $q\vec{E}$ ' represents Coulombic interactions between charges induced in the aggregates and external field. The additional force term $(\vec{p} \cdot \nabla)\vec{E}$ describes the interactions between induced dipole moments of the aggregate and a spatially inhomogeneous field [17–20]. The \vec{F}_{elec} can be considered as the net force of difference value of coulombic force and dipole moments induced interactions applied onto CNTs. With an electric field ($E = 0$), the CNTs are randomly aligned or entangled in bundle form because of strong van der Waals interactions. The oscillatory electric field applied induces quick reversing of the same and opposite charges over CNTs. When the field increases, the individual tubes in CNT bundles are aligned in the field direction to minimize dipolar energy. Therefore, beyond a certain field ($E > E_{th}$), Coulombic interaction ' $q\vec{E}$ ' surpasses van der Waals forces and CNT aggregates begin elongating along the field direction. When the field further increases ($E \gg E_{th}$), individual CNTs are stretch out from the bundle and chained through inter-CNT (dipole-dipole) interactions in the field direction as the Coulombic force ' $q\vec{E}$ ' further surpasses van der Waals forces in CNTs. Alignment behaviours are related to competition between Coulombic interactions induced by translation motions of charged CNTs and the van der Waals interactions of CNTs in CNT aggregates. According to the study on field-induced

orientation mechanisms of CNT clusters mentioned above, the key to field-induced orientation of CNTs lies in regulating strong and weak relationships between van der Waals forces and the applied electric field strength in CNTs.

The grafting of polar mesogenic segments onto the surface of m-CNTs sidewalls, as evidenced by FT-IR and XPS analyses, is mainly responsible for the uniform dispersion and field-induced orientation of m-CNTs in RMS host. On one hand, mesogenic segments are more polar and also possess larger steric hindrance than carboxylic groups [11], leading to charged m-CNTs with mesogenic groups over nanotube sidewalls to generate larger electrostatic and steric repulsion between the tubes [11,14,19] that oppose van der Waals interactions between m-CNTs. On the other hand, structural similarity between grafted mesogenic units and reactive mesogens could effectively reduce van der Waals forces between m-CNTs [11]. In addition, the electric field induced orientation effect of grafted mesogenic group also greatly improves the response ability of m-CNT for electric field in RMS media. Consequently, these analyses confirm the considerably weak π - π interactions between individual tubes in self-assembled m-CNTs result in relatively facile dispersion and orientation of m-CNTs in RMS through optical microscopy as reported in an earlier section. Therefore, due to weakened van der Waals interactions between tubes, the self-assembled m-CNTs can be easily oriented by increasing the applying field to minimize the dipolar energy and stretched to form chains through inter-CNT (dipole-dipole) interaction when the Coulombic force further surpasses van der Waals forces between CNTs. In conclusion, the 'functional LC structure' grafted onto m-CNTs can effectively regulate interactions between CNTs and LC media, improving the orientation content and efficiency of CNTs on a macroscopic scale. There is a synergistic effect between

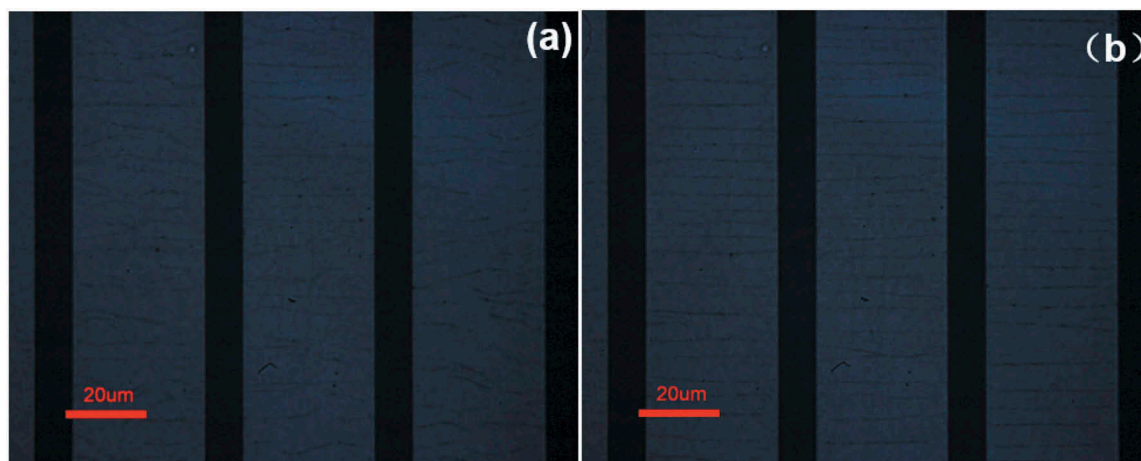


Figure 10. (Colour online) Orientation stability of aligned mesogenic CNT/RMS film without (a) and with (b) UV irradiation.

better dispersion of mesogenon-modified nanotubes and the directing effect of polymerizable mesogenic chains.

To verify the effect of UV irradiation on the orientation stability of aligned m-CNTs, the configuration of field-treated m-CNTs in RMS host with and without UV irradiation is investigated as shown in Figure 10. Interestingly, deformation in orientational ordering of m-CNTs along the horizontal direction is observed in several areas after removal of the applied field, indicating restoration of randomly entangled m-CNTs without the field in the RMS host (Figure 10(a)). Note that the stretching behaviour of this CNT sample has already been reported in previous papers [17–20], where instantaneous contraction occurs after field off. However, after UV treatment, the aligned CNTs maintain their orientation along the electric field on a macroscale, as shown in Figure 10(b), and follow a UV-induced polymerizable LC director field predetermined to be along the field direction. This indicates UV irradiation induced polymerizable chains in RMS host to surround the aligned m-CNTs and stabilized their alignment through elastic interactions with anisotropic LC media [39]. This also proves reduced van der Waals interactions between m-CNTs are mainly responsible for this behaviour.

Polarized Raman spectroscopy works well as an effective probe for checking orientation in carbon nanotubes and other highly ordered systems. The polarized Raman spectra of m-CNT/RMS composite films is obtained with two different polarizations (see Figure 11), where the polarization of the incident laser light is parallel ($V_{//}$) and perpendicular (V_{\perp}) to the direction of the CNT alignment. Generally, the intensity of the G band originating from the in-plane vibration of C = C bonds, to some

extent, reflects the orientation of m-CNT/RMS composite well [24,40]. It is found that one Raman peak appears in the range of 1585–1638 cm^{-1} and the $V_{//}$ intensity is much greater than V_{\perp} when the light is polarized parallel to the field direction, indicating the field-induced oriented m-CNTs/RMS still keeps their alignment in the hybrid film along the polymerizable mesogenic director chains. This result confirms the anisotropic orientation of the hybrid film with polarized Raman spectra.

Anisotropic light absorption properties of the hybrid film with aligned m-CNTs are evaluated in the field off-state. Figure 12 shows the polarized optical microscopy images of 4 $V_{\text{rms}}/\mu\text{m}$ field-treated m-CNTs after UV irradiation, where the polarization direction of the incident light kept parallel and perpendicular to the electric field direction. The samples prepared using m-CNT bundles are found to align along the field direction. When the transmission axis of the polarizer is kept parallel to the orientation axis of the m-CNTs, the oriented m-CNTs are obviously visible as dark lines (see Fig. 12(a)). However, the dark lines become barely visible with several traces remaining after rotating the polarizing axis of an incident light perpendicular to the orientation axis of the m-CNTs (see Figure 12(b)). As previously described, the degree of alignment of CNTs in individual bundles depends on the interaction of applied field and van der Waals interactions of nanotubes, which might be responsible for the visible traces of aligned CNT bundles at several places. This result clearly indicates that the aligned CNT bundles could absorb visible light with the electric vector ($E_{//}$) propagating along their long axis, comparatively, and the one (E_{\perp}) propagating along the short axis of the aligned CNT will pass through. The observed anisotropic light absorption of the aligned CNT bundles in prepared

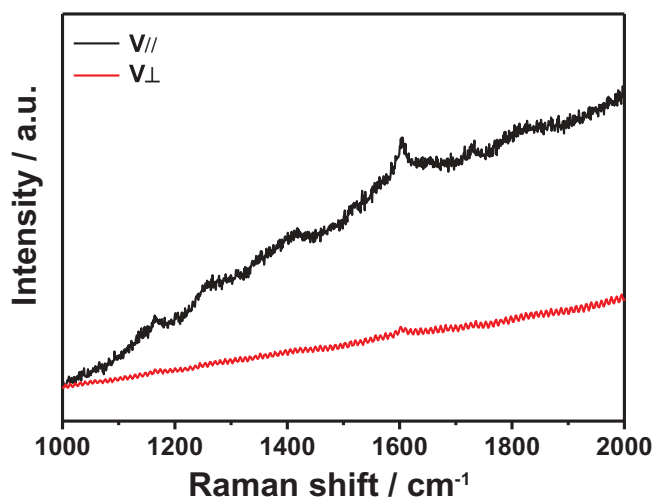


Figure 11. (Colour online) Polarized Raman spectra of aligned m-CNT/RMS hybrid films after UV irradiation. Here, the electric vector of the polarized light incident is parallel ($V_{//}$) and perpendicular (V_{\perp}) to the aligned m-CNTs.

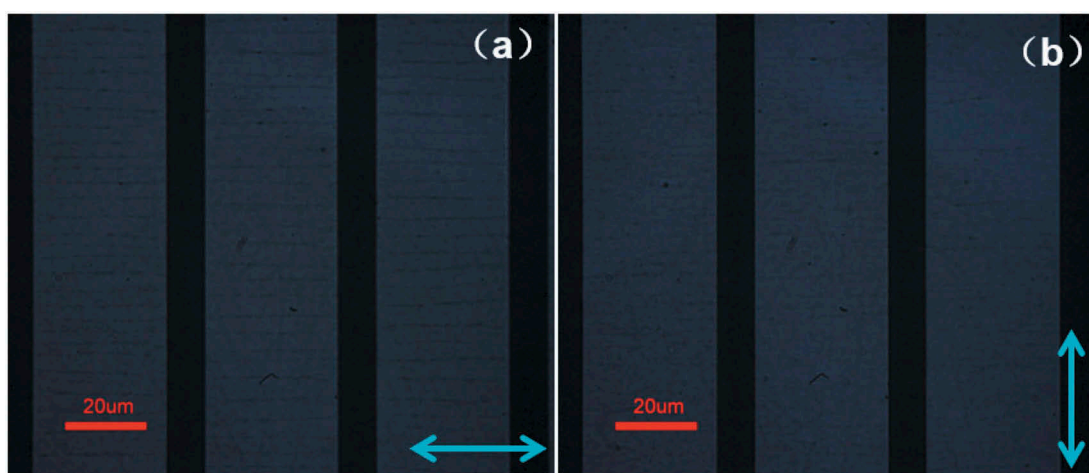


Figure 12. (Colour online) Polarized optical microphotographs of in-plane field aligned mesogenic CNTs after UV irradiation. Here, polarized visible light incident on the hybrid film with the electric vector perpendicular (a) and parallel (b) to the electrodes. The blue arrows indicate the transmission axis of the polarizer below the bottom substrate.

composite films is attributed to the optical anisotropy in extinction coefficient (α) in CNTs along and parallel to the long axis of CNTs associated optical transitions between van Hove singularities in the valence and conduction bands of CNTs [41]. Similar discussions agree with these reported analyses [18,24,41]. This further confirms the orientation ordering of the aligned CNT bundles remains stable in the field-off state after UV irradiation as discussed in the above section. Based on the anisotropic light absorption of the hybrid film, a simple light modulator utilizing m-CNT/RMS device is provided here such that an incident unpolarized light

can be polarized by the proposed film. In addition, light modulation can be performed such that an incident polarized light can be blocked or passed depending on the polarized direction of an incident light as shown in Figure 13. Novel electrically oriented polymeric film for light modulator has been developed through electric-field induced orientation (up right) of random CNT/RMS soft composite (up left) accompanied by direct ultraviolet polymerization of reactive mesogen for large scale (bottom left). Meanwhile, the orientation state of CNTs in the composites tends to be stable through curing of RMS by ultraviolet polymerization. When the electric field vector

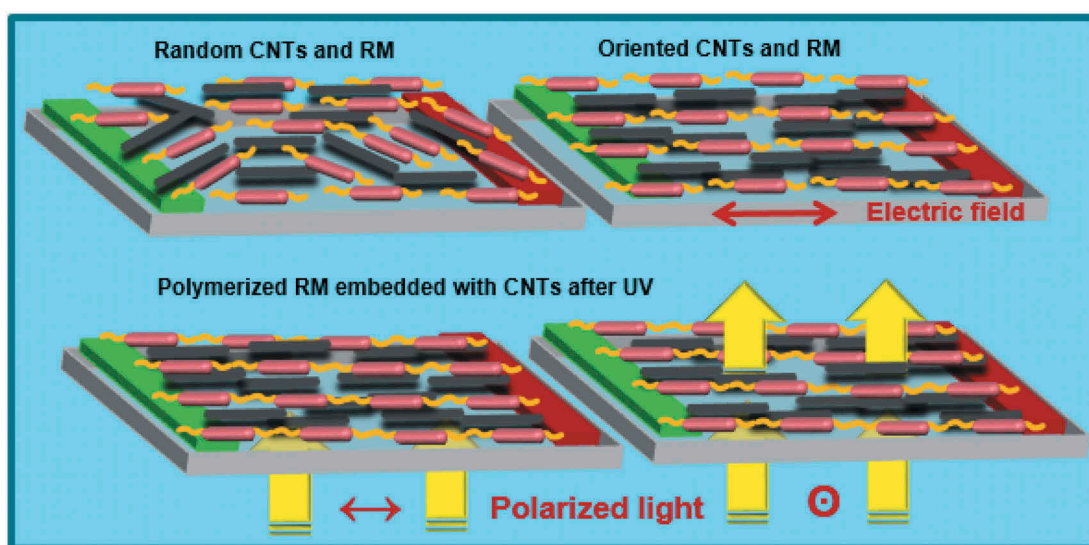


Figure 13. (Colour online) Conceived light modulator using the m-CNT/RMS device. The yellow arrows indicate the transmission axis of input polarized light parallel (left) and perpendicular (right) to the aligned hybrid film below the bottom substrate.

of an incident polarized light is either parallel (bottom left) or perpendicular (bottom right) to the uniaxially oriented liquid crystal polymer embedded with CNT, the polarized light can be either absorbed or transmitted passing through the oriented CNTs, making the device black or white. Compared with existing optoelectronic polarization devices in a polymeric film, the developed device without cross polarizers has provided new simple preparation method and theoretical basis for fabrication of well aligned and highly stabilized of CNTs based polarization-dependent devices for a large area.

4. Conclusion

We have demonstrated in-plane field-driven uniform orientation of m-CNTs in reactive mesogens that are subsequently UV-polymerized to form rigid polymeric chains, which lead to the retention of the orientation of both the mesogen molecules and nanotubes. The m-CNTs are covalently functionalized with mesogenic units via a flexible spacer on the CNT walls added through esterification between mesogenic units and carboxyl CNTs shortened to 100–500 nm in length by acid oxidation cutting. XPS and TGA analysis reveal the m-CNTs consist of a larger number of mesogenic units with flexible spacers and confirm there is better compatibility between the m-CNTs and host molecules and weaker van der Waals interactions between the m-CNTs. This gives rise to better dispersion compared to the c-CNTs, where the favourable affinity between the mesogenic moiety and host RMS molecules is responsible for the good dispersion of the m-CNTs in RMS. In addition, the orientation of the m-CNTs is controlled through an electric field and the polymerizable mesogenic director field. The aligned m-CNTs driven by electric field maintain their orientation along rigid polymeric chains in the field off-state with the assistance of anisotropic elastic interactions with the polymerizable mesogenic director field. The alignment is confirmed by polarized optic microscopy and Raman spectroscopy. More importantly, the aligned m-CNTs could absorb and transmit incident polarized visible light when axis of polarization of incident beam is propagated parallel and perpendicular to the long axis of the aligned m-CNTs, respectively. Meanwhile, the ultraviolet polymerization of reactive mesogen can be utilized to improve stabilization of the orientation of m-CNTs in the field-off state. The alignment approach of m-CNTs suggests a novel method of dynamically fixing the orientation of CNTs in polymeric film. The development of present m-CNTs contributes to fabrication of high concentration well-dispersed CNT-LC soft materials and has also provided a new method knowledge for

fabrication of highly oriented CNT structures in larger scale and high stability of CNT polarization devices.

Acknowledgments

This research was supported by the National Nature Science Foundation of China (61605167), Program for Innovative Research Team (in Science and Technology) at the University of Henan Province of China (19IRTSTHN026), Key Scientific Research Project of Universities and Colleges in Henan Province of China (17A430028), Plan for Scientific Innovation Talent of Henan Province of China (174100510014), Outstanding Young Backbone Teacher Funding Project of Xuchang University of China, and Science and Technology Bureau of Xuchang of China. Authors from CBNU acknowledge support from the Basic Research Laboratory Program (2014R1A4A1008140) through the Ministry of Science, ICT & Future Planning and (2016R1A6A3A11930056) through the National Research Foundation of Korea (NRF) funded by Ministry of Education.

Disclosure statement

No potential conflict of interest was reported by the authors.

References

- [1] Samoilov AN, Minenko SS, Lisetski LN, et al. Anomalous optical properties of photoactive cholesteric liquid crystal doped with single-walled carbon nanotubes. *Liq Cryst.* 2018;45(2):250–261.
- [2] Murakami Y, Einarsson E, Damura T, et al. Polarization dependence of the optical absorption of single-walled carbon nanotubes. *Phys Rev Lett.* 2005;94:087402.
- [3] Yang H, Fu B, Li D, et al. Broadband laser polarization control with aligned carbon nanotubes. *Nanoscale.* 2015;7:11199–11205.
- [4] Shukla RK, Chaudhary A, Bubnov A, et al. Multi-walled carbon nanotubes-ferroelectric liquid crystal nanocomposites: effect of cell thickness and dopant concentration on electro-optic and dielectric behaviour. *Liq Cryst.* 2018;45(11):1672–1681.
- [5] Vaisman L, Wagner HD, Marom G. The role of surfactants in dispersion of carbon nanotubes. *Adv Colloid Interface.* 2006;128–130:37–46.
- [6] Tie WW, Bhattacharyya SS, Park HR, et al. Comparative studies on field-induced stretching behavior of single-walled and multiwalled carbon nanotube clusters. *Phys Rev E.* 2014;90:012508.
- [7] Cole MT, Ciantanni V, Milne WI. Horizontal carbon nanotube alignment. *Nanoscale.* 2016;8:15836–15844.
- [8] Peterson MSE, Georgiev G, Atherton TJ, et al. Dielectric analysis of the interaction of nematic liquid crystals with carbon nanotubes. *Liq Cryst.* 2018;45(3):450–458.
- [9] Lagerwall JPF, Scalia G. Carbon nanotubes in liquid crystals. *J Mater Chem.* 2008;18:2890–2898.
- [10] Vigolo B, Peñicaud A, Coulon C, et al. Macroscopic fibers and ribbons of oriented carbon nanotubes. *Science.* 2000;290:1331–1334.

- [11] Jia XL, Li WS, Xu XJ, et al. Numerical characterization of magnetically aligned multiwalled carbon nanotube- Fe_3O_4 nanoparticle complex. *Appl Mater Interfaces*. 2015;7(5):3170–3179.
- [12] Remillard EM, Zhang QY, Sosina S, et al. Electric-field alignment of aqueous multi-walled carbon nanotubes on microporous substrates. *Carbon*. 2016;100:578–589.
- [13] Park JH, Kim KH, Park YW, et al. Ultralong ordered nanowires from the concerted self-assembly of discotic liquid crystal and solvent molecules. *Langmuir*. 2015;31(34):9432–9440.
- [14] Lu LH, Chen W. Large-scale aligned carbon nanotubes from their purified, highly concentrated suspension. *ACS Nano*. 2010;4(2):1042–1048.
- [15] Yao XM, Gao XY, Jiang JJ, et al. Comparison of carbon nanotubes and graphene oxide coated carbon fiber for improving the interfacial properties of carbon fiber/epoxy composites. *Composites Part B*. 2018;132:170–177.
- [16] Shoji S, Suzuki H, Zaccaria RP, et al. Optical polarizer made of uniaxially aligned short single-wall carbon nanotubes embedded in a polymer film. *Phys Rev B*. 2008;77:153407.
- [17] Jeong SJ, Park KA, Jeong SH, et al. Electroactive superelongation of carbon nanotube aggregates in liquid crystal medium. *Nano Lett*. 2007;7:2178–2182.
- [18] Tie WW, Bhattacharyya SS, Zhang YG, et al. Field-induced stretching and dynamic reorientation of functionalized multiwalled carbon nanotube aggregates in nematic liquid crystals. *Carbon*. 2016;96:548–556.
- [19] Bhattacharyya SS, Yang GH, Tie WW, et al. Electric-field induced elastic stretching of multiwalled carbon nanotube clusters: a realistic model. *Phys Chem Chem Phys*. 2011;13:20435–20440.
- [20] Kang BG, Lim YJ, Jeong KU, et al. A tunable carbon nanotube polarizer. *Nanotechnology*. 2010;2:405202.
- [21] Yaroshchuk O, Tomylo S, Kovalchuk O, et al. Liquid crystal suspensions of carbon nanotubes assisted by organically modified Laponite nanoplatelets. *Carbon*. 2014;68:389–398.
- [22] Wu Y, Cao H, Duan MY, et al. Effects of a chemically modified multiwall carbon nanotubes on electro-optical properties of PDLC films. *Liq Cryst*. 2018;45(7):1023–1031.
- [23] Kuhnast M, Tschierske C, Lagerwall JPF. Tailor-designed polyphilic promoters for stabilizing dispersions of carbon nanotubes in liquid crystals. *Chem Commun*. 2010;46:6989–6991.
- [24] Cervini R, Simon GP, Ginic-Markovic M, et al. Aligned silane-treated MWCNT/liquid crystal polymer films. *Nanotechnology*. 2008;19:175602.
- [25] Kumagai T, Yoshida H, Ozaki M. Dielectric properties of dual-frequency reactive mesogens before and after photopolymerization. *Materials*. 2014;7:1113–1121.
- [26] Zhao CG, Ji LJ, Liu HJ, et al. Functionalized carbon nanotubes containing isocyanate groups. *J Solid State Chem*. 2004;177:4394–4398.
- [27] Xing Y, Li L, Chusuei CC, et al. Sonochemical oxidation of multiwalled carbon nanotubes. *Langmuir*. 2005;21:4185–4190.
- [28] Zhang N, Sun J, Jiang DY, et al. Anchoring zinc oxide quantum dots on functionalized multi-walled carbon nanotubes by covalent coupling. *Carbon*. 2009;47:1214–1219.
- [29] Avile's F, Cauich-Rodri'guez JV, Moo-Tah L, et al. Evaluation of mild acid oxidation treatments for MWCNT functionalization. *Carbon*. 2009;47:2970–2975.
- [30] Zhang XD, Cong YH, Zhang BY. Covalent modification of reduced graphene oxide by chiral side-chain liquid crystalline oligomer via Diels-Alder reaction. *RSC Adv*. 2016;6:96721–96728.
- [31] Xue YH, Liu Y, Lu F, et al. Functionalization of graphene oxide with polyhedral oligomeric silsesquioxane (POSS) for multifunctional applications. *J Phys Chem Lett*. 2012;3:1607–1612.
- [32] Tune DD, Stolz BW, Pfohl M, et al. Dry shear aligning: a simple and versatile method to smooth and align the surfaces of carbon nanotube thin films. *Nanoscale*. 2016;8:3232–3236.
- [33] Liang CZ, Wang B, Chen JJ, et al. Dispersion of multi-walled carbon nanotubes by polymers with carbazole pendants. *J Phys Chem B*. 2017;121:8408–8416.
- [34] Pacheco FG, Cotta AAC, Gorgulho HF, et al. Comparative temporal analysis of multiwalled carbon nanotube oxidation reactions: evaluating chemical modifications on true nanotube surface. *Appl Sur Sci*. 2015;357:1015–1023.
- [35] Datsyuk V, Guerret-Piécourt C, Dagréou S, et al. Double walled carbon nanotube/polymer composites via in-situ nitroxide mediated polymerisation of amphiphilic block copolymers. *Carbon*. 2005;43:873–876.
- [36] Cha JM, Jin SG, Shim JH, et al. Functionalization of carbon nanotubes for fabrication of CNT/epoxy nanocomposites. *Mater Des*. 2016;95:1–8.
- [37] Sánchez-López JC, Donnet C, Lefèbvre F, et al. Bonding structure in amorphous carbon nitride: a spectroscopic and nuclear magnetic resonance study. *J Appl Phys*. 2001;90:675–681.
- [38] Longin NL, Nikolai IL, Sergei VN, et al. Dispersions of multi-walled carbon nanotubes in liquid crystals: a physical picture of aggregation. *J Mol Liq*. 2011;164:143–147.
- [39] Basu R, Kinnamon D, Garvey A. Nano-electromechanical rotation of graphene and giant enhancement in dielectric anisotropy in a liquid crystal. *Appl Phys Lett*. 2015;106:201909.
- [40] Yoo HJ, Lee SY, You NH, et al. Dispersion and magnetic field-induced alignment of functionalized carbon nanotubes in liquid crystals. *Synth Met*. 2013;181:10–17.
- [41] Landi BJ, Ruf HJ, Evans CM, et al. Purity assessment of single-wall carbon nanotubes, using optical absorption spectroscopy. *J Phys Chem B*. 2005;109:9952–9965.